4-20-1999

The PG X-Ray QSO Sample: Links between the Ultraviolet-X-Ray Continuum and Emission Lines

Beverley J. Wills
University of Texas at Austin

A. Laor
Technion-Israel Institute of Technology, Israel

M. S. Brotherton
Lawrence Livermore National Laboratory

D. Wills
University of Texas at Austin

B. J. Wilkes
Harvard University

See next page for additional authors

THE ASTROPHYSICAL JOURNAL, 515:L53–L56, 1999 April 20

THE PG X-RAY QSO SAMPLE: LINKS BETWEEN THE ULTRAVIOLET–X-RAY CONTINUUM AND EMISSION LINES

BEVERLEY J. WILLS,[1] A. LAOR,[2] M. S. BROTHERTON,[3] D. WILLS,[1] B. J. WILKES,[4] G. J. FERLAND,[5] AND ZHAOHUI SHANG[1]

Received 1999 January 14; accepted 1999 February 18; published 1999 March 10

ABSTRACT

Two sets of relationships relate QSO UV to soft X-ray continua with the broad-line region. These are (i) the Baldwin relationships, which are inverse relationships between the broad-line equivalent width and the continuum luminosity, and (ii) Boroson & Green's optical "Principal Component 1" relationships, linking steeper soft X-ray spectra with narrower Hβ emission, stronger Hβ blue wings, stronger optical Fe II emission, and weaker [O III] λ5007 lines. In order to understand these relationships, we extended the spectra into the UV for 22 QSOs with high-quality soft X-ray spectra. These are from the complete sample of QSOs from the Bright Quasar Survey for which Laor et al. demonstrated strong luminosity and X-ray–optical Principal Component 1 relationships. We show that these extend to a whole new set of UV relationships: Principal Component 1 (in the sense of steeper X-ray spectra) is related to narrower C III] λ1909 lines, larger Si III] λ1892/C III] λ1909 ratios (a high-density indicator), stronger low-ionization lines, and weaker C IV λ1549 but stronger N V λ1240 lines. We speculate that high accretion rates are linked to high columns of dense ($\sim 10^{11}$ cm^{-3}), nitrogen-enhanced, low-ionization gas from nuclear starbursts. Line width, inverse Fe II–[O III] and inverse Fe II–C IV relationships hint at the geometrical arrangement of this gas. These Principal Component 1 relationships appear to be independent of luminosity and therefore of the Baldwin relationships.

Subject headings: accretion, accretion disks — galaxies: starburst — quasars: emission lines — quasars: general — ultraviolet: galaxies — X-rays: galaxies

1. INTRODUCTION

The UV to soft X-rays of luminous active galactic nuclei (AGNs) dominate their bolometric luminosity, powered by accretion onto a massive black hole at the center. The release of energy within a few gravitational radii determines the spectral energy distribution at optical photon energies and above. These photons illuminate and ionize the surrounding gas on subparsec to kiloparsec scales—the fuel and exhaust of the central engine. In addition to photoionization, two sets of relationships, neither of which are understood, link central engine properties with the structure, dynamics, and physical conditions of the surrounding gas. One is the Baldwin effect in the UV (Baldwin et al. 1978), and the other is the X-ray–optical "Principal Component 1" (PC1) relationships presented by Boroson & Green (1992, hereafter BG92) and Laor et al. (1994 and 1997a, hereafter L94 and L97, respectively). Optical PC1, accounting for most of the spectrum-to-spectrum variation in low-redshift AGN samples, is a linear combination of observables: as Hβ from the broad-line region (BLR) becomes narrower, its profile changes from having a stronger red wing to one having a stronger blue wing; the strength of BLR Fe II (optical) emission increases; [O III] λ5007 narrow-line region (NLR) emission decreases; the optical–X-ray and X-ray spectra steepen; and X-ray variability increases (increasing α_{ox} and α_x, where $F_\nu \propto \nu^{-\alpha}$) (BG92; L94; L97; Grupe et al. 1998; Fiore et al. 1998).

In order to investigate these relationships closer to the central engine, we have extended, into the UV, the spectra of 22 QSOs[6] from the same complete, optically selected sample of 23 PG QSOs investigated by L94 and L97. They selected all QSOs from the Bright Quasar Survey (Schmidt & Green 1983) with $z < 0.4$ and a Galactic hydrogen columns of $N_{\mathrm{H}\,i} < 1.9 \times 10^{20}$ cm^{-2}. The low redshift allowed Laor et al. to detect soft X-ray emission (0.15–2 keV) down to the lowest possible rest-frame energies (<0.2 keV) and, for our study, allowed access to emission lines over a wide ionization range, but with minimal intervening intergalactic absorption. The low Galactic hydrogen column and the accurate 21 cm measurements of this column ensured small, accurate corrections for absorption in both the X-ray and UV regions. Here we present a remarkable new set of relationships extending the PC1 relationships into the UV, further linking QSO spectral energy distributions with the properties of the emitting gas (see also Wills et al. 1999a, 1999b, 1999c).

2. OBSERVATIONS AND MEASUREMENTS

We obtained *Hubble Space Telescope* (*HST*) Faint Object Spectrograph (FOS) spectrophotometry for 16 QSOs and used archival FOS data for six QSOs, from wavelengths below Lyα to beyond 3200 Å. Resolutions are ~230 km s^{-1} (FWHM). Most optical data are from BG92. Figure 1 displays representative UV spectra in the order of the *X-ray–optical* PC1, with steeper soft X-ray spectra and stronger Fe II (optical) at the top.

We measured strengths, ratios, and widths (FWHM) for Lyα, N V λ1240, the λ1400 feature (Si IV, O IV] blend), C IV λ1549, Al III λ1860, Si III] λ1892, and C III] λ1909. Care was taken to robustly deblend these prominent lines from nearby contaminating features, and the details will be given by Wills et al.

[1] McDonald Observatory and Department of Astronomy, RLM 15.308, University of Texas at Austin, TX 78712; bev@astro.as.utexas.edu.

[2] Department of Physics, Technion–Israel Institute of Technology, Haifa, 32000, Israel.

[3] Institute of Geophysics and Planetary Physics, P.O. Box 808, L-413, Lawrence Livermore National Laboratory, Livermore, CA 94550-9900.

[4] Harvard-Smithsonian Center for Astrophysics, 60 Garden Street, Cambridge, MA 02138.

[5] University of Kentucky, Department of Physics and Astronomy, 177 Chemistry/Physics Building, Lexington, KY 40506-0005.

[6] One object was omitted for nonscientific reasons, so this omission does not bias the sample.

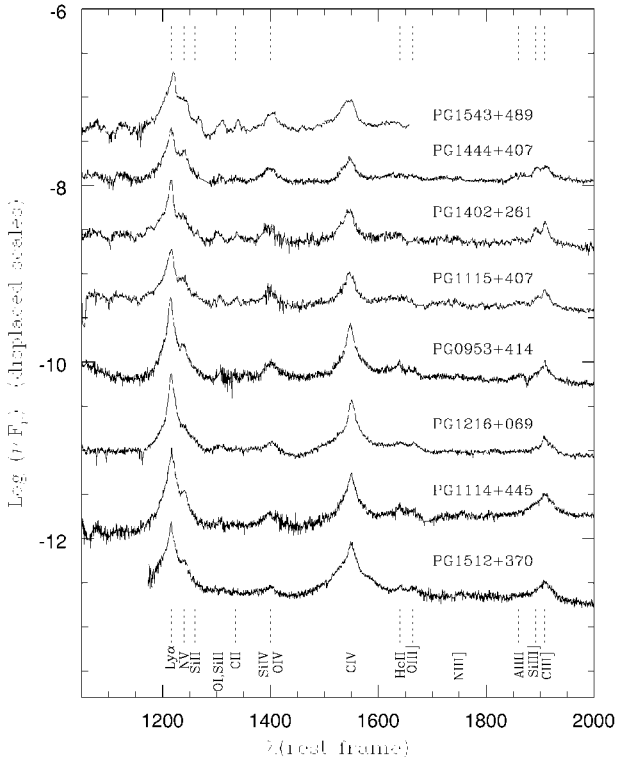

FIG. 1.—Selected *HST*-FOS spectra of PG QSOs plotted on a logarithmic flux-density scale in the order of the optical–X-ray PC1, with the QSOs at the top having the steepest X-ray spectra. Increasing upward, notice the increasing prominence of Al III λ1860, Si III] λ1892, O I λ1304, and C II λ1335. The λ1400 blend of O IV] and Si IV, as well as the apparent strength of N V λ1240 increase relative to C IV and Lyα, are shown.

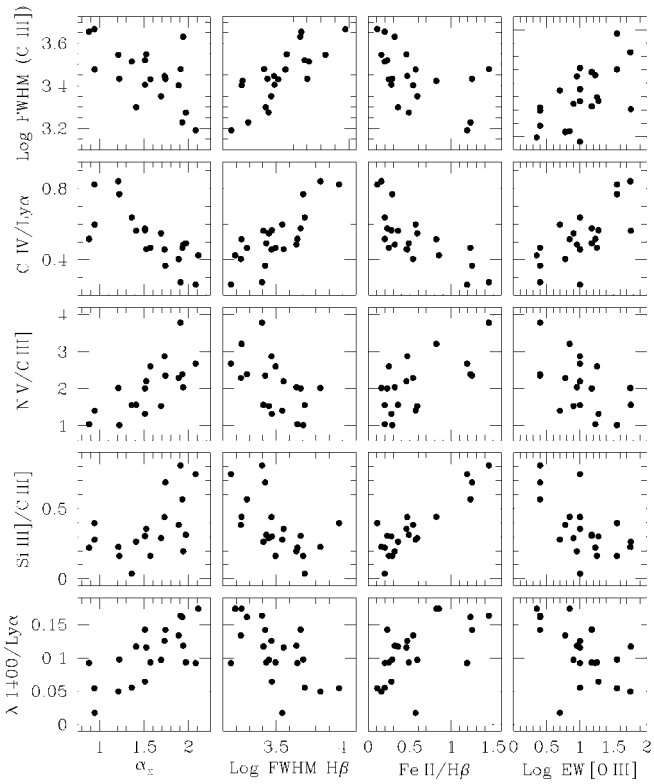

FIG. 2.—UV observables vs. α_x and optical PC1 observables. Many line ratios are consistent with these trends—lower ionization and higher densities, in addition to (not shown) weaker [O III] λ5007 from the NLR—all corresponding to steeper soft X-ray spectra. The two-tailed probability of these correlations, arising by chance from unrelated variables, is between one in 50 and one in $\gg$1000.

(1999c). In most cases, we used our McDonald Observatory spectra to define a "rest-frame" wavelength scale that was referred to [O III] λ5007 from the NLR. The greatest uncertainties in the line measurements arise from uncertainties in continuum placement and in the removal of associated and Galactic interstellar absorption. Some actual line measurements are tabulated by Francis & Wills (1999).

3. CORRELATIONS

Some of the most important correlation results are summarized in Table 1 and Figure 2. Column (1) of Table 1 lists emission-line parameters of the UV spectrum: line ratios and logarithms of rest-frame equivalent width (EW) and line width (FWHM). Columns (2)–(6) give correlation coefficients for the UV parameters versus the well-known PC1 parameters, α_x derived from a fit between 0.2 and 2 keV (L97), and parameters of the optical spectrum as given by BG92. Column (7) gives correlation coefficients between the UV parameters of column (1) and a linear combination of X-ray–optical PC1 parameters derived from a principal components analysis of our sample (see below and Francis & Wills 1999). Figure 2 plots some of the correlations of Table 1, i.e., the four columns representing X-ray–optical PC1 observables: the steepness of the X-ray

TABLE 1

CORRELATION COEFFICIENTS[a]

		Optical First Principal Component Parameters					
UV Parameters (1)	α_x (2)	FWHM Hβ (3)	EW Fe II (4)	Fe II/Hβ (5)	EW [O III] (6)	Optical–X-Ray PC1 (7)	L_{1216} (8)
FWHM C III]	**−0.56**	**0.78**	**−0.41**	**−0.58**	0.18	**−0.57**	−0.27
EW Lyα	−0.20	0.25	−0.04	−0.17	0.30	−0.19	**−0.65**
EW C IV	**−0.48**	**0.69**	**−0.60**	**−0.66**	**0.65**	**−0.69**	−0.26
C IV/Lyα	**−0.72**	**0.66**	**−0.63**	**−0.68**	**0.56**	**−0.74**	0.23
EW C III]	−0.32	**0.44**	−0.35	−0.39	0.37	−0.39	**−0.60**
Si III]/C III]	**0.54**	**−0.66**	**0.66**	**0.71**	**−0.54**	**0.71**	−0.13
Si III]/Lyα	**0.46**	**−0.70**	**0.74**	**0.80**	**−0.67**	**0.78**	−0.28
N V/C III]	**0.76**	**−0.62**	**0.68**	**0.57**	**−0.48**	**0.76**	0.09
N V/Lyα	**0.58**	**−0.43**	**0.54**	**0.48**	**−0.60**	**0.64**	0.04
λ1400/Lyα	**0.62**	**−0.58**	**0.60**	**0.59**	**−0.57**	**0.70**	−0.20

[a] The Spearman rank correlation coefficients are given, with the most significant shown in boldface. For 22 QSOs, a correlation coefficient of 0.4 corresponds to one chance in 15 of arising from uncorrelated variables (two-tailed), 0.5 corresponds to one chance in 50, 0.6 to one chance in 300, and 0.7 to one chance in 2000.

TABLE 2
PRINCIPAL COMPONENTS ANALYSIS[a]

Parameter	PC1	PC2	PC3
Eigenvalue	6.49	2.47	1.63
Proportion	0.499	0.190	0.126
Cumulative	0.499	0.689	0.815
L_{1216}	0.01	0.52	−0.30
α_x	0.32	−0.16	0.03
FWHM Hβ	−0.35	0.03	−0.32
Fe II/Hβ	0.35	−0.09	0.09
EW [O III]	−0.30	0.02	0.25
FWHM C III]	−0.20	−0.06	−0.61
EW Lyα	−0.15	−0.51	0.10
EW C IV	−0.33	−0.24	0.05
C IV/Lyα	−0.34	0.18	0.03
EW C III]	−0.25	−0.47	−0.08
Si III]/C III]	0.35	−0.06	−0.02
N V/Lyα	+0.23	−0.14	−0.54
λ1400/Lyα	0.23	−0.31	−0.24

[a] There were 18 QSOs used in this analysis. L_{1216} represents continuum luminosity at 1216 Å.

spectrum, the width of the broad Hβ line, the strength of Fe II (optical), and the strength of NLR emission ([O III] λ5007).

The X-ray–optical PC1, increasing in the sense of softer X-ray spectrum, extends to the UV, corresponding to narrower C III] emission and stronger low-ionization lines (Fe III, Si III] λ1892, Al III λ1860, and others; Fig. 1), but also, surprisingly, to stronger, higher ionization lines of N V λ1240 and the λ1400 blend (Si IV and O IV]). The ratio Si III] λ1892/C III] λ1909 increases, and the C III] λ1909 EW decreases—most simply interpreted as collisional suppression of C III] λ1909 in gas with densities $\gtrsim 10^{10.5}$ cm^{-3}—indicating either increasing gas density or an increasing fraction of higher density gas (see, e.g., Laor et al. 1997b). The strength of C IV λ1549 is inversely correlated with the strength of Fe II (optical) (Wang, Zhou, & Gao 1996) and is correlated with [O III] (Brotherton 1999). Fe III UV 34 (λ1895, λ1914, and λ1926) also contributes more when Fe II is strong. Mrk 478, in our sample, and I Zw 1 (Laor et al. 1997b) have especially soft X-ray spectra, especially strong Fe II (optical), as well as strong Fe III (I Zw 1 did not meet the Galactic obscuration criteria for inclusion in the sample but is otherwise eligible.) As expected, the UV parameters show very significant correlations among themselves. The strongest correlations that we have found should and do show up by inspection of Figure 1.

Complementary to the direct correlations is our principal components analysis (PCA). Table 2 shows the results of a PCA performed on the ranked variables, giving the projection of the input variables on the first three principle components. Half of the sample variance (49.9%) is described by a linear combination of variables related to the X-ray–optical PC1 found by BG92, L94, and L97. We now have an X-ray–UV–optical PC1.

Table 1 also shows correlations between UV emission-line parameters and L_{1216}, the log of the continuum luminosity at 1216 Å (col. [8]). The Baldwin relationships are present for Lyα, C IV λ1549, and C III] λ1909 (Fig. 3); no Baldwin relationship is found for Hβ, [O III] λ5007, or Fe II (optical), which is in agreement with other investigations. An interesting result is that neither the new UV variables nor the original X-ray–optical PC1 appear to depend on luminosity at all (correlation coefficients ~0.1): the Baldwin relationships appear to be independent of the X-ray–UV–optical PC1. This is in accordance with Table 2, in which PC2 accounts for 19% of the variance and is dominated by Baldwin relationships. C IV λ1549 is significant in both PC1 and PC2, probably accounting for its weaker Baldwin relationship in our sample (Fig. 3).

PC3 appears to represent an independent relationship between luminosity and line widths. Such correlations have been previously interpreted in terms of gravitational dynamics and black hole mass (see, e.g., Joly et al. 1985; Wandel 1991; Laor 1998), as both velocities and luminosities may be expected to increase with increasing mass.

4. DISCUSSION

The most important result is *the spectacular set of related correlations that we have found among many variables*. Some individual correlations have been found before in large, heterogeneous samples: Fe II (optical) versus λ1400/C IV and C IV/Lyα, and α (UV–X-ray) versus C IV/Lyα (Wang et al. 1996; Wang, Lu, & Zhou 1998); the Fe II–Si III]/C III] relationships, as well as the Al III/C III] and Fe III/C III] relationships, have very recently also been noted by Aoki & Yoshida (1999). Brotherton (1999) gives an independent presentation of the C IV–[O III] relationship, and Wills et al. (1993) have shown the inverse relation between the strength of C IV and the λ1400 feature.

The X-ray–emission-line relationships provide plausibly strong links between the central engine parameters and the kinematics, geometry, and physics of fueling gas or outflows on subparsec to kiloparsec scales.

1. In principle, line widths (profiles), together with BLR distances based on echo-mapping time delays or dust-sublimation radii, may be used to infer the virial central masses, hence $L_{\rm Edd}$ (Peterson et al. 1998; Laor 1998). QSO luminosities

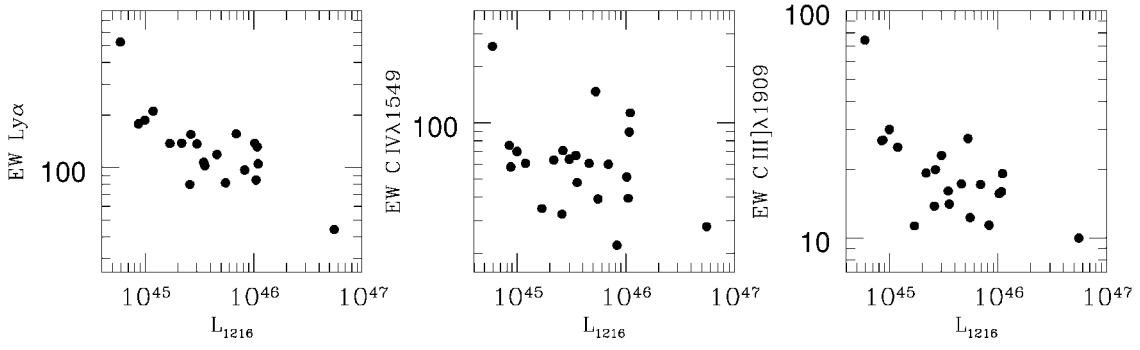

FIG. 3.—The Baldwin relationships for Lyα, C IV λ1549, and C III] λ1909 for ~20 QSOs of the PG X-ray sample

often appear to be significant compared with L_{Edd}, suggesting that accretion onto a central black hole could be an unstable process, giving rise to winds.

2. The widths of Hβ and C III] λ1909 are related to α_x, linking kinematics directly to a central engine property. By analogy with Galactic black hole candidates in their "high" states, steep X-ray spectra may be related to high accretion rates (Pounds, Done, & Osborne 1995).

3. The structure of the BLR must be linked to α_x and hence probably to accretion and outflowing winds. One possible explanation for the inverse Fe II–[O III] relation is that the smaller the effective covering of the central engine by optically thick BLR gas, the more photons are available to ionize the more distant NLR (BG92; Brotherton 1999). If the strong inverse C IV–Fe II (optical) relations has a similar explanation, then significant low-velocity C IV–emitting gas lies beyond an Fe II–emitting BLR shield. This would tie in with Brotherton's result: C III] and C IV emission from lower velocity gas is correlated with [O III] emission from the NLR.

4. High-ionization N V λ1240 also appears to be associated with high-density gas. N V increases while C IV decreases with increasing PC1 (i.e., steeper soft X-ray spectrum and stronger Fe II). This apparent anomaly is reminiscent of the behavior of the N V Baldwin relation (Espey 1999) in which the slope of the Baldwin relation for several other species is tightly correlated with ionization potential, but for N V, the EW dependence on luminosity is much less than expected. Korista, Baldwin, & Ferland (1998) show that the EW N V–luminosity relationship can be understood if very nitrogen-rich gas (Hamann & Ferland 1993) is irradiated by a UV–to–soft X-ray continuum that becomes softer with increasing luminosity. While this is a complex issue, perhaps our N V anomaly can be similarly explained by enhanced nitrogen abundances.

The "mystery physics" underlying all the Principal Component 1 relationships could be an increase in L/L_{Edd} associated with an increase in dense, Fe II–emitting gas of high metallicity. It has been suggested that the QSO's with extreme low-ionization spectra and strong Fe II are also undergoing starbursts (Lîpari, Terlevich, & Macchetto 1993). Could starburst activity cause increased accretion of enriched gas and hence strong soft X-rays?

We gratefully acknowledge the help of C. D. Keyes and A. Roman of STScI, M. Dahlem (now of ESTEC), and also M. Cornell and R. Wilhelm, who provided computer support in the Department of Astronomy of the University of Texas. This research is supported by NASA through LTSA grant NAG5-3431 (B. J. W.) and grant GO-06781 from the Space Telescope Science Institute, which is operated by the Association of Universities for Research in Astronomy, Inc., under NASA contract NAS5-26555. M. S. B.'s research has been performed under the auspices of the US Department of Energy by the Lawrence Livermore National Laboratory under contract W-7405-ENG-48. We have used the NASA/IPAC Extragalactic Database (NED), which is operated by the Jet Propulsion Laboratory, California Institute of Technology, under contract with the National Aeronautics and Space Administration.

REFERENCES

Aoki, K., & Yoshida, M. 1999, in ASP Conf. Ser. 162, Quasars and Cosmology, ed. G. Ferland & J. Baldwin (San Francisco: ASP), in press (astro-ph/9812364)
Baldwin, J. A., Burke, W. L., Gaskell, C. M., & Wampler, E. J. 1978, Nature, 273, 431
Boroson, T. A., & Green, R. F. 1992, ApJS, 80, 109 (BG92)
Brotherton, M. S. 1999, in preparation
Espey, B. R. 1999, in ASP Conf. Ser. 162, Quasars and Cosmology, ed. G. Ferland & J. Baldwin (San Francisco: ASP), in press
Fiore, F., Laor, A., Elvis, M., Nicastro, F., & Giallongo, E. 1998, ApJ, 503, 607
Francis, P. J., & Wills, B. J. 1999, in ASP Conf. Ser. 162, Quasars and Cosmology, ed. G. Ferland & J. Baldwin (San Francisco: ASP), in press
Grupe, D., Beuermann, K., Mannheim, K., & Thomas, H.-C. 1998, A&A, submitted
Hamann, F., & Ferland, G. J. 1993, ApJ, 418, 11
Joly, M., Collin-Souffrin, S., Masnou, J. L., & Nottale, L. 1985, A&A, 152, 282
Korista, K., Baldwin, J., & Ferland, G. J. 1998, ApJ, 507, 24
Laor, A. 1998, ApJ, 505, L83
Laor, A., Fiore, F., Elvis, M., Wilkes, B., & McDowell, J. C. 1994, ApJ, 435, 611 (L94)
Laor, A., Fiore, F., Elvis, M., Wilkes, B., & McDowell, J. C. 1997a, ApJ, 477, 93 (L97)
Laor, A., Jannuzi, B. T., Green, R. F., & Boroson, T. A. 1997b, ApJ, 489, 656
Lîpari, S., Terlevich, R., & Macchetto, F. 1993, ApJ, 406, 451
Peterson, B. M., Wanders, I., Bertram, R., Hunley, J. F., Pogge, R. W., & Wagner, R. M. 1998, ApJ, 501, 82
Pounds, K. A., Done, C., & Osborne, J. P. 1995, MNRAS, 277, L5
Schmidt, M., & Green, R. F. 1983, ApJ, 269, 352
Wandel, A. 1991, A&A, 241, 5
Wang, T.-G., Lu, Y.-J., & Zhou, Y.-Y. 1998, ApJ, 493, 1
Wang, T.-G., Zhou, Y.-Y., & Gao, A.-S. 1996, ApJ, 457, 111
Wills, B. J., Brotherton, M. S., Fang, D., Steidel, C. C., & Sargent, W. L. W. 1993, ApJ, 415, 563
Wills, B. J., Brotherton, M. S., Laor, A., Wills, D., Wilkes, B. J., Ferland, G. J., & Shang, Z. 1999a, in ASP Conf. Ser. 162, Quasars and Cosmology, ed. G. Ferland & J. Baldwin (San Francisco: ASP), in press
———. 1999b, in Structure and Kinematics of Quasar Broad Line Regions, ed. C. M. Gaskell, W. N. Brandt, M. Eracleous, M. Dietrich, & D. Dultzin-Hacyan (San Francisco: ASP), in press
Wills, B. J., et al. 1999c, in preparation